IJCRT.ORG ISSN : 2320-2882

INTERNATIONAL JOURNAL OF CREATIVE RESEARCH THOUGHTS (IJCRT)

An International Open Access, Peer-reviewed, Refereed Journal

Zns/Rgo Composite Via Co-Precipitation For Inactivation Of Malachite Green And Pathogens

D Varaprasad[a], B Sathish Mohan[b,*], Dharmasoth Ramadevi[c,d], K Basavaiah[a,*], P.Vani[a]

[a]Dept of Inorganic & Analytical Chemistry, Andhra University, Visakhapatnam 530003, India.

[b]Bio Enviro Chemical Solutions, Visakhapatnam 530017, India.

[c]AU College of Pharmaceutical sciences, Andhra University, Visakhapatnam 530003, India.

[d]Samuel George Institute of Pharmaceutical sciences, Markapur, Andhra Pradesh 523316, India.

Abstract

The current study describes the preparation of reduced graphene oxide based zinc sulphide (ZnS-RGO) composite *via* co-precipitation approach and different composites were prepared with the changing in concentration of GO. The obtained samples were examined for their structural, optical and electrical properties of prepared samples with the help of sophisticated analytical instruments such as XPS, FTIR, XRD, BET, SEM-EDX, TEM, UV-DRS and TGA. The prepared composites and pure ZnS and its composites were determined for their photocatalytic performance by the degradation of malachite green dye aqueous solution under visible light irradiations. Significant result obtained as a complete degradation of MG dye aqueous solution in 180 min by ZnS-RGO composite with the optimized pH-9, 0.03g catalyst dosage and 10 ppm dye concentration. In addition, the antibacterial performance of prepared composites were determined over the gram positive and negative bateiral pathogens and results drawn that prepared composite was the most effective for the degradation of malachite green and antibacterial agent.

Keywords

ZnS-RGO; co-precipitation; malachite green; photocatalytic degradation; antimicrobial activity.

1. Introduction

Dyeing and drug industries releases dye pollutants and pathogens (bacteria and fungi) into aquatic system, forms water pollution [1]. The wastewater is a significant source of aesthetic contamination, eutrophication and perturbation in aquatic life. Therefore, treatment of wastewater is needed before further processing to minimize the pollution to ecosystem [2]. Nowadays, researcher's attention towards advanced oxidation processes (AOPs) includes photo fenton, ozonization, UV/H_2O_2 fenton, and semiconductor based photocatalysis i.e. carried out in presence of light (UV, Visible or sunlight) help of semiconductors have been acquired great attention [3-4]. In that sense, semiconductor metal oxides involvement is much great and have been reported as efficient photocatalysts for environmental abatement applications [5].

Zinc sulfide (ZnS) is II-VI group semiconductor photocatalyst owing to the rapid formation of electron and hole pair [6-7]. ZnS has a wide bandgap energy of 3.2 eV which means it captures more UV light like well-known other semiconductor photocatalyst TiO_2 [8]. A drawback of ZnS is wider bandgap energy which leads to the fast recombination rate of charge carriers of electrons and holes by absorption of UV light (wavelength 380 nm) and resulting lesser photocatalytic activity. Therefore, ZnS has more probabilities to use as photocatalyst in visible light for degradation of dye pollutants effectively [9-10]. To increase the photocatalytic performance of blend ZnS is by either doping or composite with other narrow bandgap materials that could be a promising material for removal of dye pollutants and microorganisms from their contaminated water.

Among various photocatalysts, the composites of reduced graphene oxide (RGO) with semiconductors are of significant relevance since they have suitable optical and physicochemical properties like solar light harvesting tendency, great stability, great photocharge separation efficacy and excellent adsorption of pollutants from aqueous solutions [11]. Graphene based materials have been extensively studied because of their remarkable bactericidal performance in broad applications in photocatalysis and antimicrobial activity [12-13]. Hence, RGO based composites can have greater photocatalytic efficacy towards the degradation of dye pollutants and pathogens removal. Recently, RGO based binary, ternary and quaternary composites have been developed over the last two decades [14-15]. This paper discusses the role of RGO loading on photocatalytic degradation of Malachite green (MG) dye aqueous solution under visible light irradiations. Moreover, the possible mechanism of photocatalytic degradation of model dye pollutant like Malachite green using the proposed ZnS-RGO composite Furthermore, the plausible photocatalytic pathway for the generation of free radicals by RGO-based composites is also explained in detail. Also, study the inactivation of pathogens by prepared ZnS and its composites. This study will be beneficial to the researchers in field of materials science for developing new metal sulfides based RGO composites as superior photocatalysts and benign antimicrobial agents.

2. Experimental section

2.1 Materials

Graphite flakes, sodium nitrate ($NaNO_3$), sulfuric acid (H_2SO_4), zinc nitrate ($Zn(NO_3)_2$), hydrogen peroxide (H_2O_2), ethanol (C_2H_5OH) hydrochloric acid (HCl), ammonium sulphate ($(NH_4)_2SO_4$), sodium hydroxide (NaOH), and sodium borohydride ($NaBH_4$) were procured from Sigma Aldrich Company, India and used without further purification. The malachite green was received from Merck chemical Ltd, India, used without further purification and Milli Q water was used in all preparing solutions.

2.2 Methodology

Synthesis of desirable composite

In a facile synthesis of MnS_2-RGO composite, initially, the pre-weighed amount of GO was sonicated for 1h. In another beaker, the 40 mL of $Zn(NO_3)_2$ (0.25M), 25 mL of ethanol and 30 mL of $(NH_4)_2SO_4$ (0.1M) were taken, allowing for 1h stirring. The GO was added to the above solution and a pinch of $NaBH_4$ was also added. This solution was mixed for 3h continuously with a controlled temperature of 90 ^oC. After completion of the reaction, the mixture solution was cooled to reach room temperature and then washed several times with ethanol followed by water. Finally, the obtained brown coloured product was filtered and dried overnight in a hot air stabilizer at 70 ^oC. In absence of GO, the ZnS nanoparticles were synthesized by following the same procedure.

Preparation of GO

Universal modified Hummer's method was adopted to obtain GO. For that, 3g of graphite flakes were sonicated for 30 minutes before oxidation. Then, sonicated graphite (1 g) and $NaNO_3$ (0.5 g) were suspended in 69 ml concentrated sulphuric acid in an ice bath (to maintain the temperature below 5 ^oC) in a 500 ml round bottom flask under gentle magnetic stirring for 15 min. Then 3 g of $KMnO_4$ was added continuously pinch by pinch by keeping the temperature of the solution did not exceed 20 ^oC. Then, the ice bath was removed and stirred the solution at 35 ^oC under a reflux condenser for 3 hours. After that, 130 ml of distilled water was added and stirring continued for an additional one hour. Excess unreacted $KMnO_4$ was removed by 10 ml of 30% H_2O_2. The complete removal of $KMnO_4$ was indicated by a colour change from dark to yellow. As prepared GO was carefully washed with deionised water several times and dried overnight in the oven at 70 ^oC.

2.3 Characterization

The prepared catalysts were further characterized using analytical instruments in a detail, microscopic studies were conducted on SEM and TEM to study morphology with elemental composition by EDX analysis. The crystallinity of the compound was studied using XRD patterns using Bruker AXS D8 Advance X-ray diffractometer with Cu-kα wavelength at the scan rate speed of 0.02 ^{o}/C. The functional groups on the catalyst surface were determined using FTIR analysis (IR prestige 21, Shimadzu) in the range from 500 to 4000 cm^{-1}. XPS (PHI 5000 versaprobe III) and UV-visible spectrophotometer (Shimadzu 2600R) were used to study the optical properties of prepared samples in the wavelength of 200 to 800 nm. TGA analysis was performed using TG100 with a scanning temperature of 28-1000 ^{o}C. BET analysis performed using BELSORP MiniII in presence of N_2 and He gas.

2.4 Dye degradation experiment

The photocatalytic performance of prepared samples (ZnS and ZnS-RGO composites) was executed by experimenting with malachite green (MG). A well-designated photoreactor with a visible lamp and magnetic stirrer was used for this purpose. The initially desirable concentration was prepared and the same was taken into a 250 mL beaker and the pre-weighed catalyst amount was added to it. The mixture solution is stirred for 30 min to optimize the adsorption of MG dye molecules on the surface of the catalyst. Then, light is allowed and extends for till decolourise the solution. The aliquots were collected at regular time intervals, which further allowed obtaining UV-Vis spectral analysis for measuring the degradation rate. The percentage of the degradation rate of MG dye aqueous solution was measured through A_t-A_o/A_t x 100, A_t and A_o are the absorbance at a time 't' and initial time of MG dye solution respectively.

2.5 Antibacterial activity

The Bacterial cultures are grown overnight at 37^{o}C temperature were used for testing the antibacterial activity. Nutrient agar medium (High media) was dissolved in the water this was distributed in a 100ml conical flask and was sterilized in an autoclave at 121^{o}C 15lbp for 15min after autoclaved the media poured sterilized petriplates. Chloramphenicol was taken as a positive control for antibacterial activity. The antibacterial activity of the compound was evaluated by Agar well diffusion method (Perez et al., 1990). Inoculums were spread over the surface of agar plates with a sterile glass spreader. Four wells were made at an equal distance using a sterile cork borer. To examine the antibacterial activity of the compounds were made final concentrations of 40mg/ml, 60µg/ml, 80µg/ml of extract were poured on each well and then plates were incubated for a period of 24h at 37 ^{o}C in an incubator after incubation diameter (mm) of the clear inhibitory zone formed around the well was measured.

3. Results and discussion

3.1 XRD spectral analysis

Fig.1 describes the XRD patterns of prepared samples (ZnS and ZnS/RGO composites) via co-precipitation approach. However, the prepared ZnS and its composites with RGO shows the diffraction patterns at (2θ=) 29.2°, 48.5° and 57° which assigned the respective planes of (111), (220) and (311) represents the cubic phase of ZnS [16]. Evident that prepared composites have great crystal change is GO converted into RGO by the absence of respective GO peak usually appeared at (2θ=) 10°. The average crystalline size of prepared composites and blend ZnS were measured using Debey-Scherrer's equation [17]

$$D = k\lambda / \beta \cos\theta \qquad \text{Eq (1)}$$

Here, Scherer constant is 'k' (0.9), 'λ' is the wavelength (0.154 nm Cu-Kα radiations), 'β' is the full width at half maximum (FWHM) and θ is incident angle of the X-rays. The analysis results confirmed that prepared ZR-2 composite have lesser in average crystalline size (23 nm) compared to ZR-1 composite (29.6 nm) and pure ZnS (33.9 nm). Lesser size particles possess greater photocatalytic performance so ZR-2 composite may exhibit maximum degradation rate.

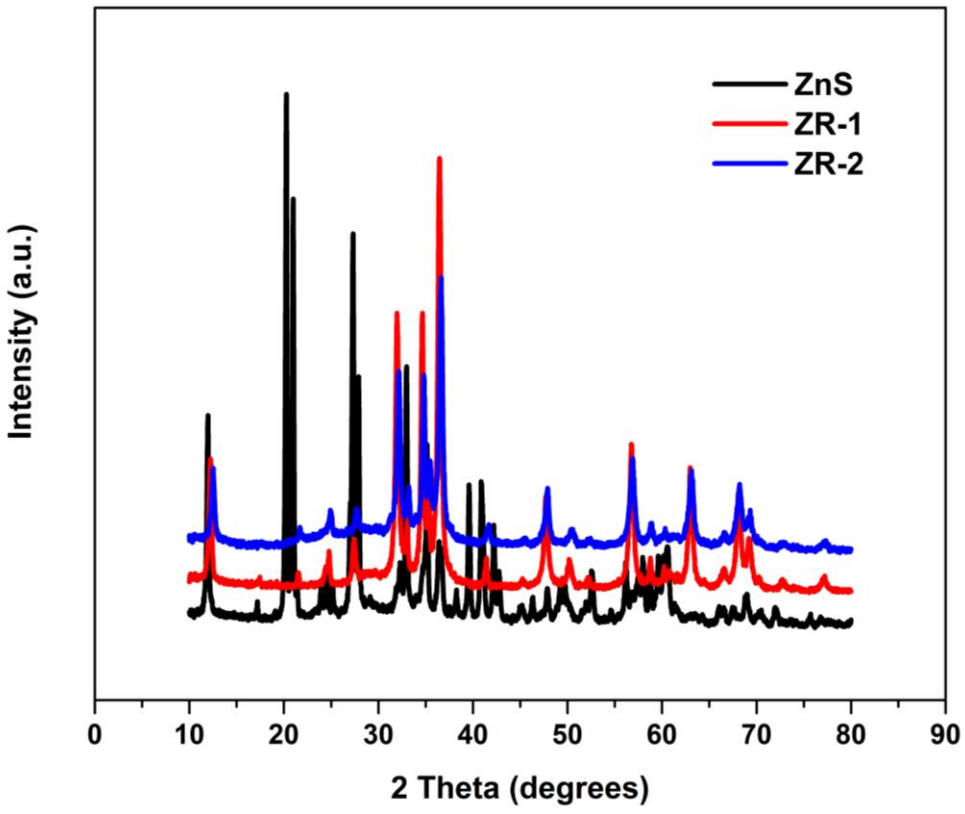

Fig.1: XRD patterns of prepared ZnS and ZnS-RGO composites

3.2 XPS analysis

Connection with elemental analysis from EDX analysis, XPS assay was used to extend the analysis of elemental existence presented on the surface of the prepared samples. Fig.2 displays the analysis results showed the XPS peaks at 1021, 528, 285 and 168 eV for elements such as Zn 2p3/2, O 1s, C 1s and S 2p respectively means a purest desirable compound is formed via co-precipitation approach.

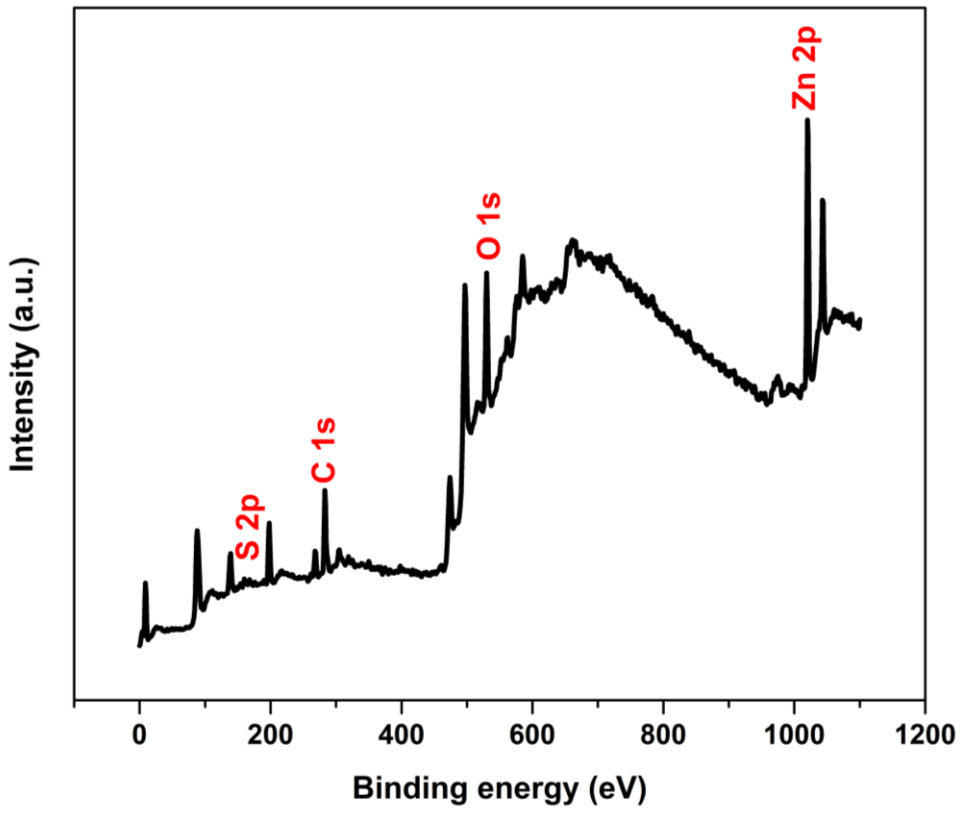

Fig.2: XPS spectrum of prepared composite ZnS-RGO

3.3 FTIR study

The prepared ZnS and ZnS-RGO composites were further characterized by FTIR and the results are presented in Fig.3. A prominent broad peak was located at 3417 cm^{-1} owing to the existence of quinazoline or vasicine alkaloids which accountable for the capping of prepared composites prevent the agglomeration. And this peak indicated the transformation of GO into RGO (represents the O-H group of the hydrated molecule). The SO_4^{2-}, C-O and C=C groups also noticed in prepared composites and the respective peaks located at 709, 1103, 1688 and cm^{-1} respectively [16-17].

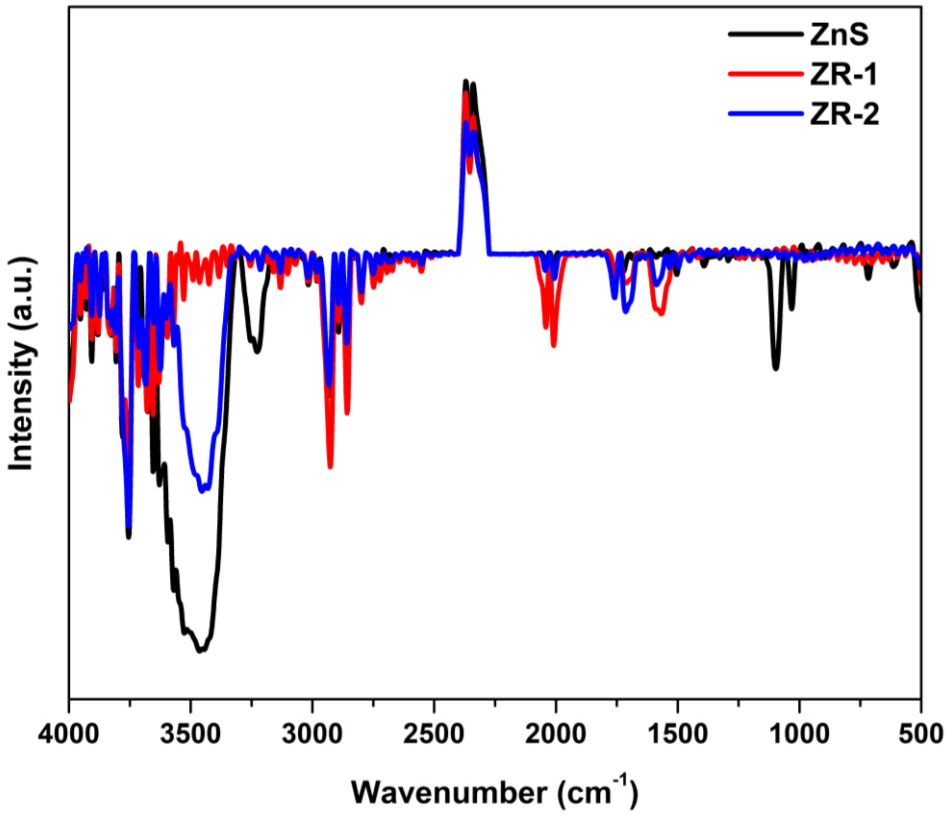

Fig.3: FTIR spectra of prepared samples

3.5 TGA study

Fig.4 shown the thermal behaviour of prepared pure ZnS and ZnS-RGO composites was carried out by the Thermogravimetric analysis (TGA). All samples were heated up to 1000^{o} C with the heating rate of 10^{o} C/min. As an evident, from the TGA results, ZR-1 composite possesses greater thermal stability (24%) than other ZR-2 composite (33%) and ZnS (36%). Due to demoisture, a slight thermal decay was observed in all produced. The next weight loss step was occurred above 250^{o} C, this might be owing to the sublimation of metal sulphides.

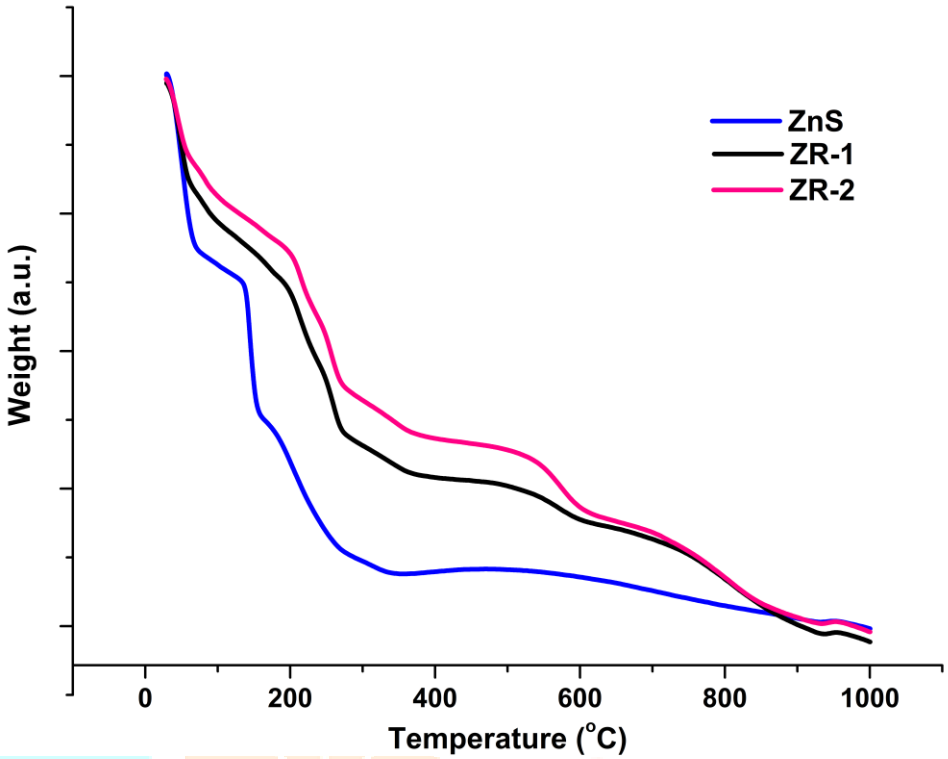

Fig.4: TGA images of prepared ZnS and ZnS-RGO composites

3.6 Optical properties analysis

The optical absorption property results in better photocatalytic activity. The bandgap energy of prepared materials was determined using the Tauc plot equation as Eq 2.

$$\alpha h\upsilon = A\,[h\upsilon - Eg]n/2 \qquad \text{Eq (2)}$$

Where 'α' is the absorption coefficient, 'A' is the constant and 'n' indices indirect (n = ½) or direct (n = 2) bandgap material. Also 'E_g' is bandgap energy, and 'λ' is wavelength corresponding to the absorption edge.

The absorption peak of ZR composite was slightly shifted to visible region, i.e. red (Fig.5). This represents the maximum visible light captured by composite and exhibits the better photocatalytic activity. Lesser the bandgap material exhibited good photocatalytic activity [1]. The analysis results found that prepared ZR-2 and ZR-1 composites shows 2.8 eV which is lower than other materials such as 3.2 eV for both MR-1 and ZnS respectively. Based on this, the ternary composite acted as best photocatalyst for dye degradation under visible light radiations due to it falls in the visible region. UV-Visible spectrometer analysis is performed in this study to determine the optical properties of prepared ZnS and ZnS-RGO composites (ZR-1 and ZR-2). Fig.6 displays the UV-Vis absorption spectra of prepared samples show the electrons excitation at 367 nm except ZnS.

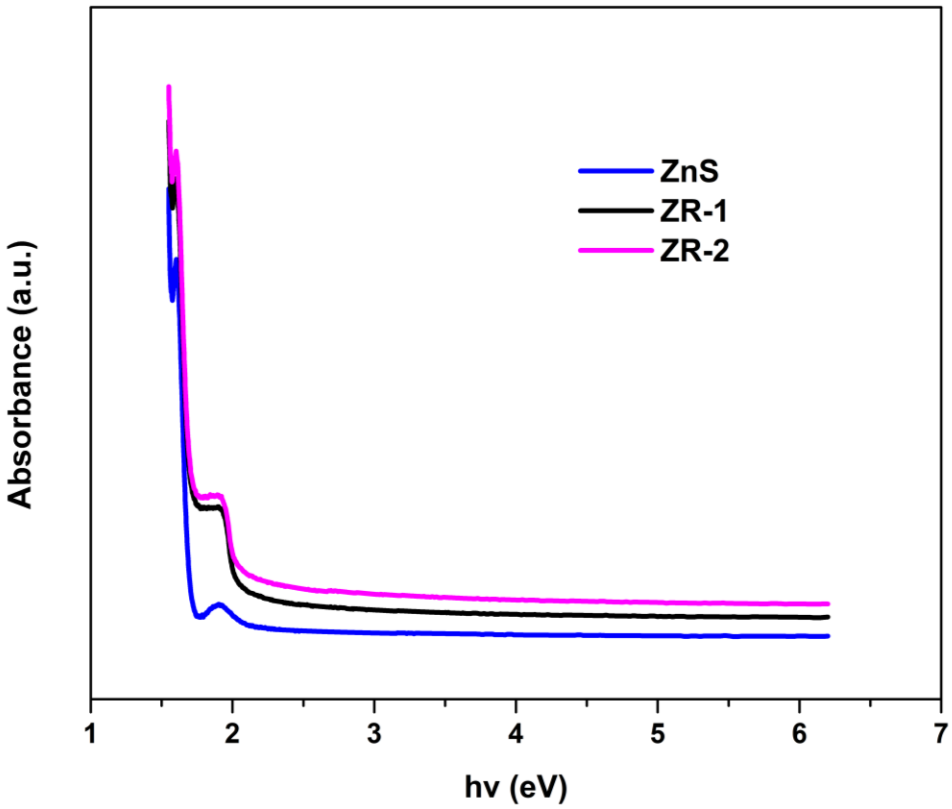

Fig.5: UV-DRS spectra of prepared ZnS and ZnS-RGO composites

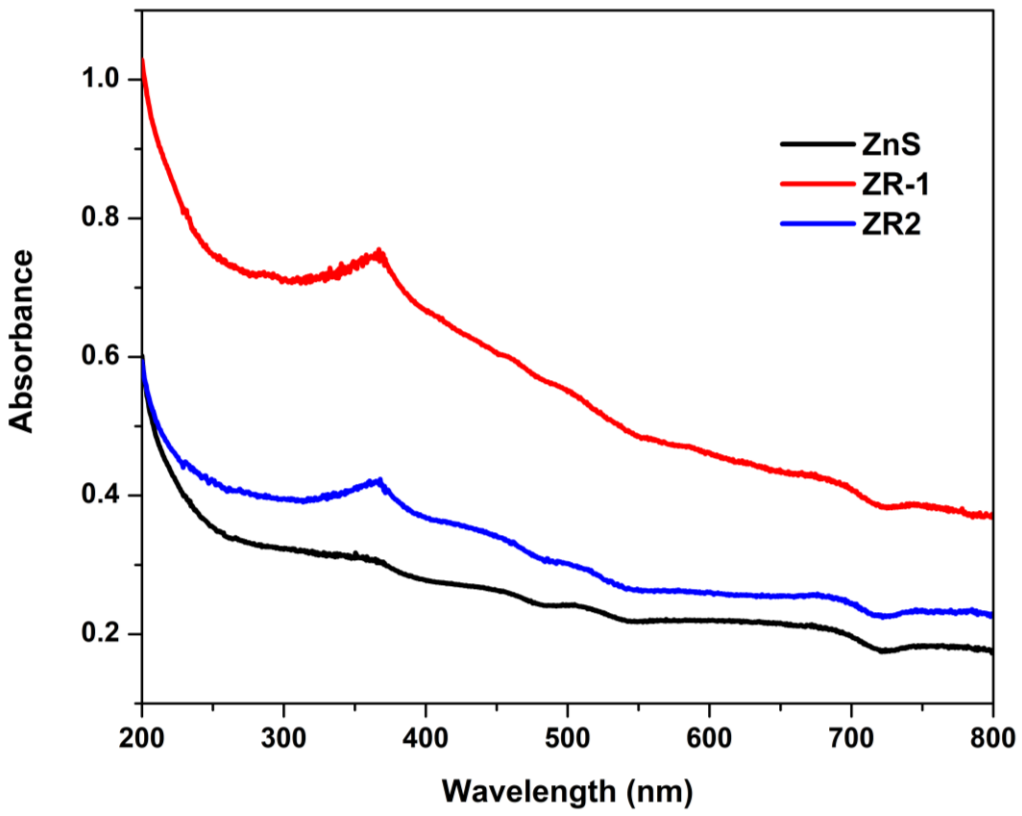

Fig.6: UV-Vis spectral analysis of prepared ZnS and ZnS-RGO composites

3.7 Morphology study

Structure and morphology of prepared samples were determined using SEM (scanning electron microscopy) and TEM (Transmission electron microscopy). Fig.7. implies the TEM, SAED (selected area electron diffraction) and histogram images of prepared ZnS-RGO composite. The obtained composite shows the great agglomeration (can seen in a) with high crystallinity due to the RGO in composite [18]. From histogram distribution curve the average particle size of prepared composite was measured using ImageJ and found that 24 nm which is coherent with XRD results.

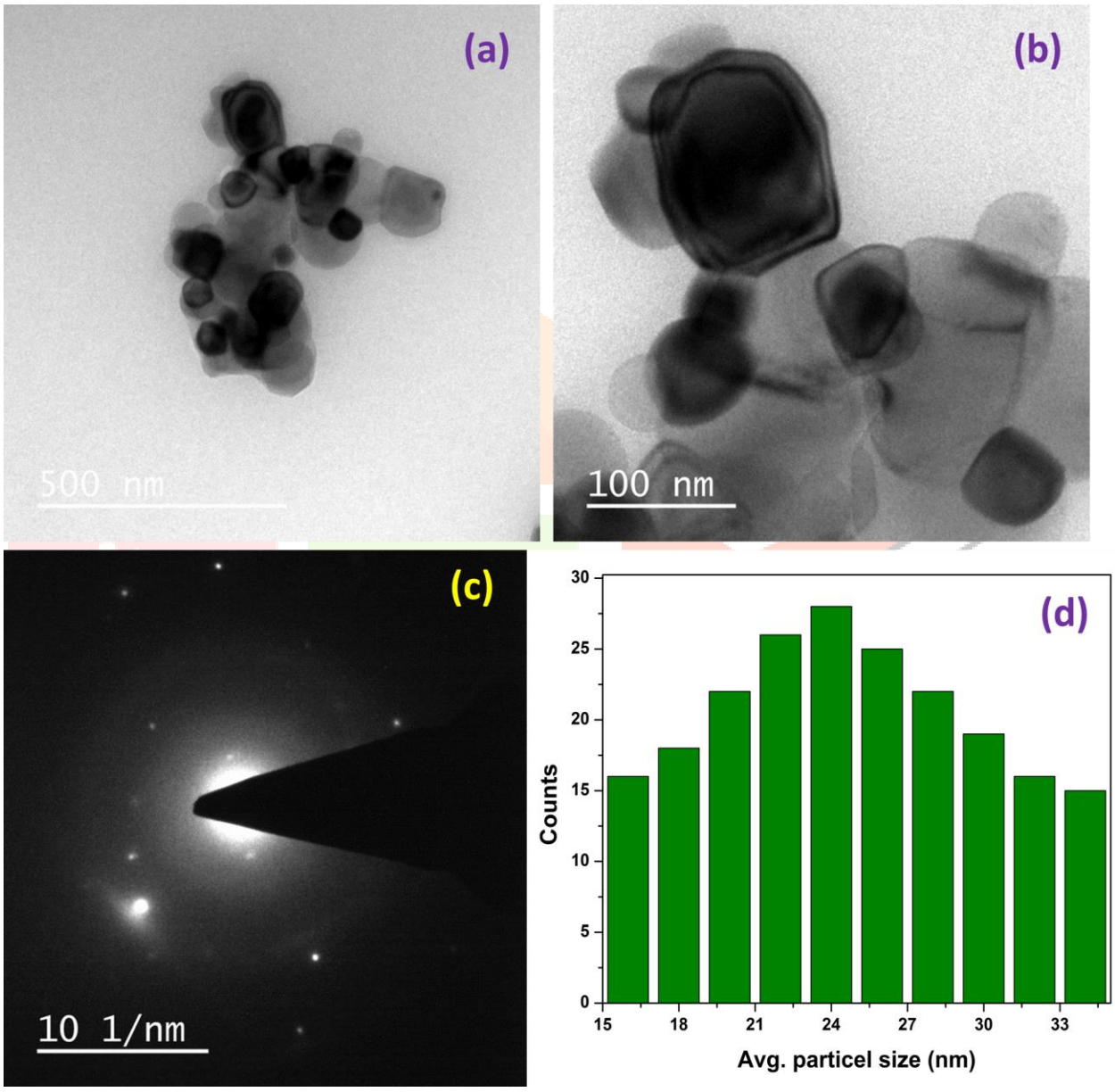

Fig.7: (a,b) TEM images, (c) SAED and (d) histogram distribution curve of prepared samples

Further morphology of prepared samples (ZnS, ZR-1 and ZR-2 composites) *via* co-precipitation approach was studied by scanning electron microscopy (SEM) with the range of 1µm to 200 nm. Noticed that co-precipitation route approach favours the fine morphology of prepared samples are formed. Fig.8 interprets the SEM images of ZnS and composites which are in spherical shape with uniformity. Also noticed that bare ZnS lies on the surface of layers of RGO that have reached out more aggregation as p-p interactions over RGO layers [18].

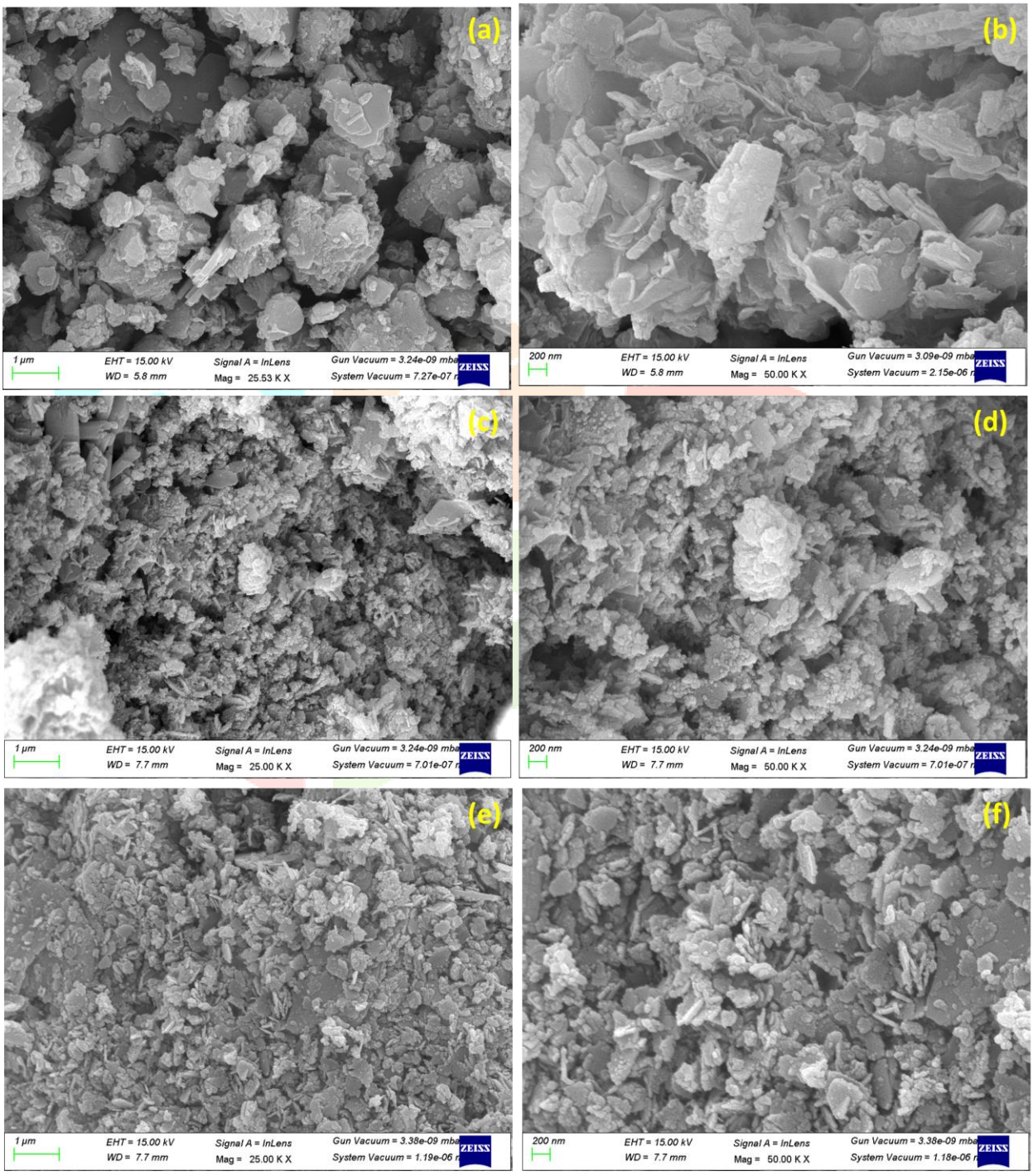

Fig.8: SEM micrographs of prepared (a,b) ZnS, (c,d) ZR-1 and (e,f) ZR-2 composites

The elemental analysis of the prepared composite was studied using energy dispersive x-ray spectroscopy (EDX). Fig.9 exhibits the peaks of elements such as Zinc (Zn), sulphur (S), carbon (C), and oxygen (O) evident the purest form of ZnS-RGO composite is formed with no impurities.

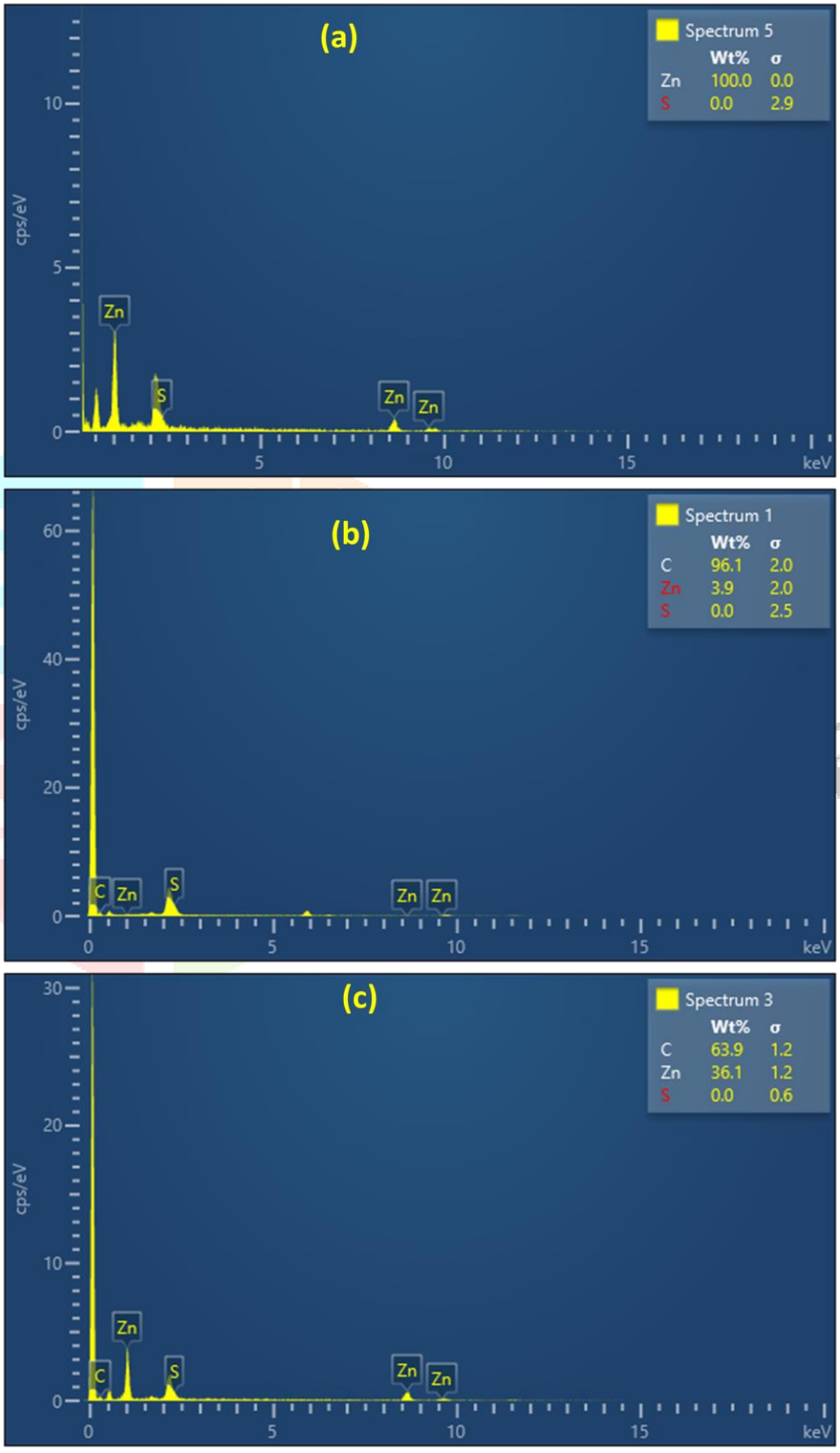

Fig.9: EDX analaysis of prepared (a) ZnS, (b) ZR-1 and (c) ZR-2 composites

Photocatalytic degradation studies

The photocatalytic activity of synthesized ZnS and ZnS-RGO composites was studied in the degradation of malachite green (MG) dye aqueous solution under visible light illumination. Based on recent literature on photocatalytic degradation of MG dye aqueous solution under visible light irradiations and optimize the experimental conditions such as pH, catalyst amount and dye concentration solution. Initially, the prepared ZnS was tested under vigorous conditions such as 0.03g of catalyst and 10 ppm of dye aqueous solution (basic) as per literature and exhibited moderate degradation rate 63% in 180 min. So, the addition of GO to metal sulfide my lead better photocatalytic efficiency compared to results obtained from pure metal sulfide. To evident this statement, ZR-1 composite showed maximum degradation rate (86% in 180 min) towards the photocatalytic degradation of MG dye aqueous solution under visible light illumination as shown in Fig.10. ZR-2 composite also possess greater photocatalytic performance in 180 min is a complete decolourisation of MG dye aqueous solution under visible light irradiations.

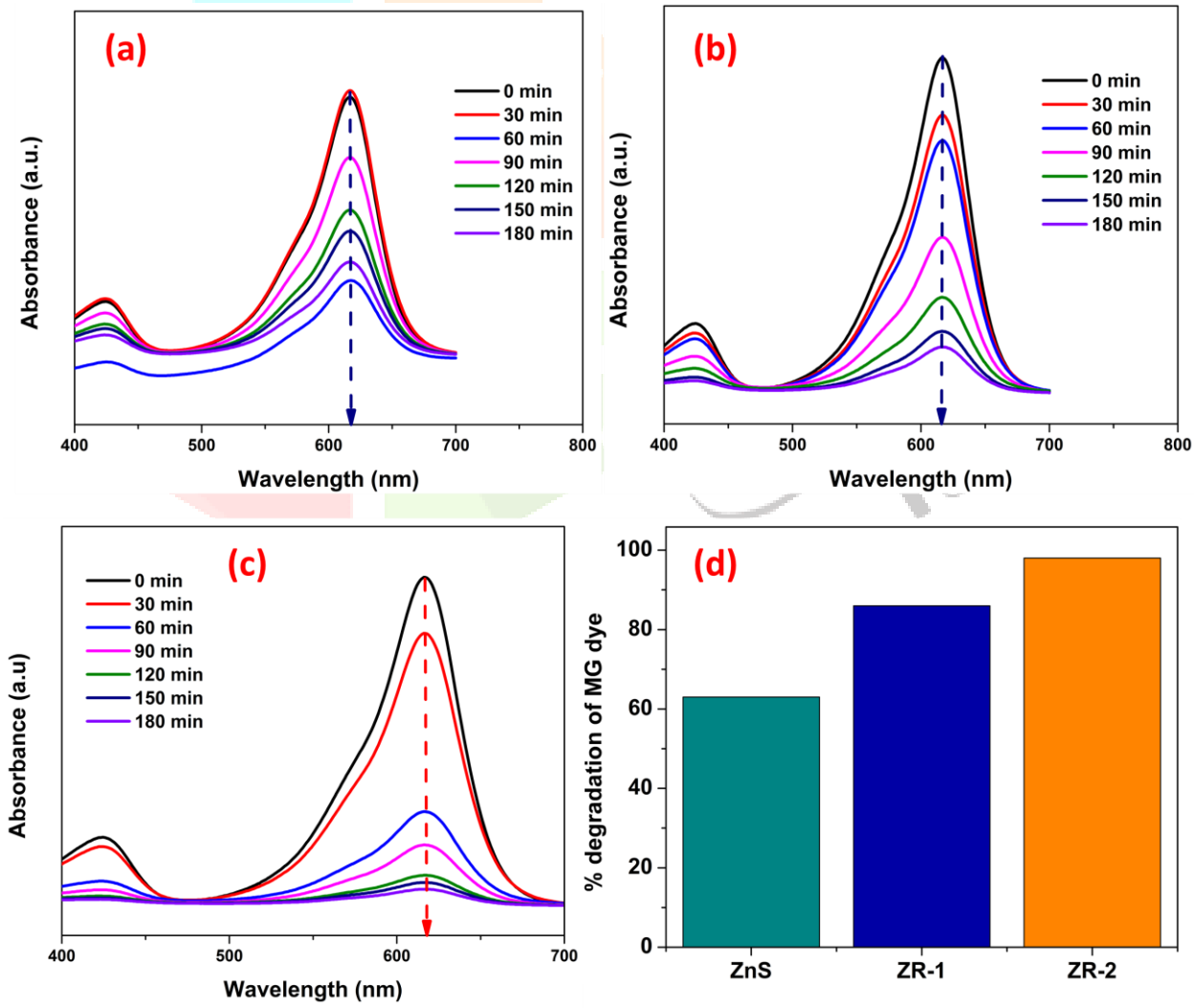

Fig.10: Photocatalytic degradation of MG dye by prepared (a) ZnS, (b) ZR-1, (c) ZR-2 composites and (d) overall degradation efficiency

Proposed mechanism

A plausible mechanism of photocatalytic degradation performance of prepared ZnS-RGO composite under visible light irradiations is schematically illustrated in Fig.11. The ZnS-RGO nanocomposite is kept in visible light illumination; initially, MnS_2 undergoes a charge separation process that leads to the promotion of electrons from the valence band (VB) to the conduction band (CB) and leaving a hole in the VB. Due to the formation of heterojunction, the photogenerated electrons in CB of MnS_2 transferred to CB of ZnS. Meanwhile, the excited holes at the valence band (VB) of MnS_2 were transferred to the VB of ZnS. Finally, the photogenerated electrons are captured by the RGO sheets through semiconductor carbon heterojunction which dramatically enhanced photogenerated charge separation efficiency in ZnS-RGO nanocomposite. Simultaneously an equal amount of holes have been formed in semiconductor nanocomposite. These separated electrons and holes directly react with oxygen and water to generate highly reactive superoxide radicals ($^{\bullet}O_2^-$) and hydroxyl radicals ($^{\bullet}OH$). These energetic reactive radicals consequently react with surface adsorbed nitrophenols molecules and degraded them into small intermediate molecules, such as CO_2 and H_2O. Based on the above mechanism explanation for photocatalytic degradation of dye in the presence of ZnS-RGO nanocomposite under visible light irradiation was shown by the following equations (3-10).

$ZnS + h\nu \longrightarrow (e^-) + (h^+)$ Eq.3

$ZnS\ (h^+) + H_2O \rightarrow {}^{\bullet}OH + H^+$ (4)

$ZnS\ (e^-) + RGO \rightarrow RGO\ (e^-) + MnS_2$ (5)

$RGO\ (e^-) + O_2 \longrightarrow RGO + {}^{\bullet}O_2^-$ (6)

$H_2O + {}^{\bullet}O_2^- \longrightarrow HO_2^{\bullet} + OH^-$ (7)

$2HO_2^{\bullet} \longrightarrow H_2O_2 + O_2$ (8)

$H_2O_2 + {}^{\bullet}O_2^- \longrightarrow OH^- + {}^{\bullet}OH + O_2$ (9)

$^{\bullet}OH/{}^{\bullet}O_2^-/ HO_2^{\bullet} + dye \longrightarrow$ Degradation products Eq.10

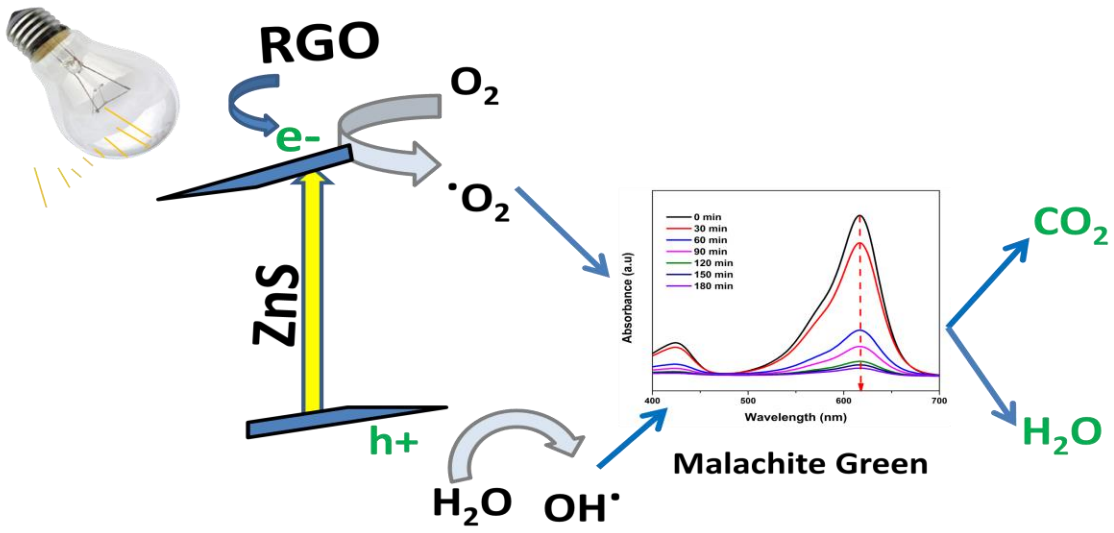

Fig.11: Photocatalytic degradation of MG dye using ZnS-RGO composite

The synthesized reduced graphene oxide based metal sulfide composite showed better photocatalytic activity due to increases in the number of impurity energy levels between the VB and CB which helps for the generation of more electron-hole pairs, thus decreasing the recombination of photogenerated holes and electrons by reduced graphene oxide [1-3] to eliminate the harmful effect of defect bands.

Recycling and stability of photocatalyst

The prepared composite was further examined for its recyclability and stability towards the degradation of malachite green (MG) dye aqueous solution. In that sense, the used photocatalyst was collected after completion of the degradation experiment. The collected photocatalyst was washed thoroughly with water followed by the ethanol, centrifuged and finally dried for further degradation experiment. A remarkable degradation rate was achieved by reused photocatalyst, and the same experiment pursues up to five cycles. The degradation rate decreased gradually and reached 80 % at the fifth cycle due to the weight loss of photocatalyst during the washing (Fig.12). After recycling the photocatalyst, it is further examined for its sustainability by characterizing it with XRD. There is no change in the XRD planes of the tested photocatalyst, which means it is stable for up to five cycles as shown in Fig.13.

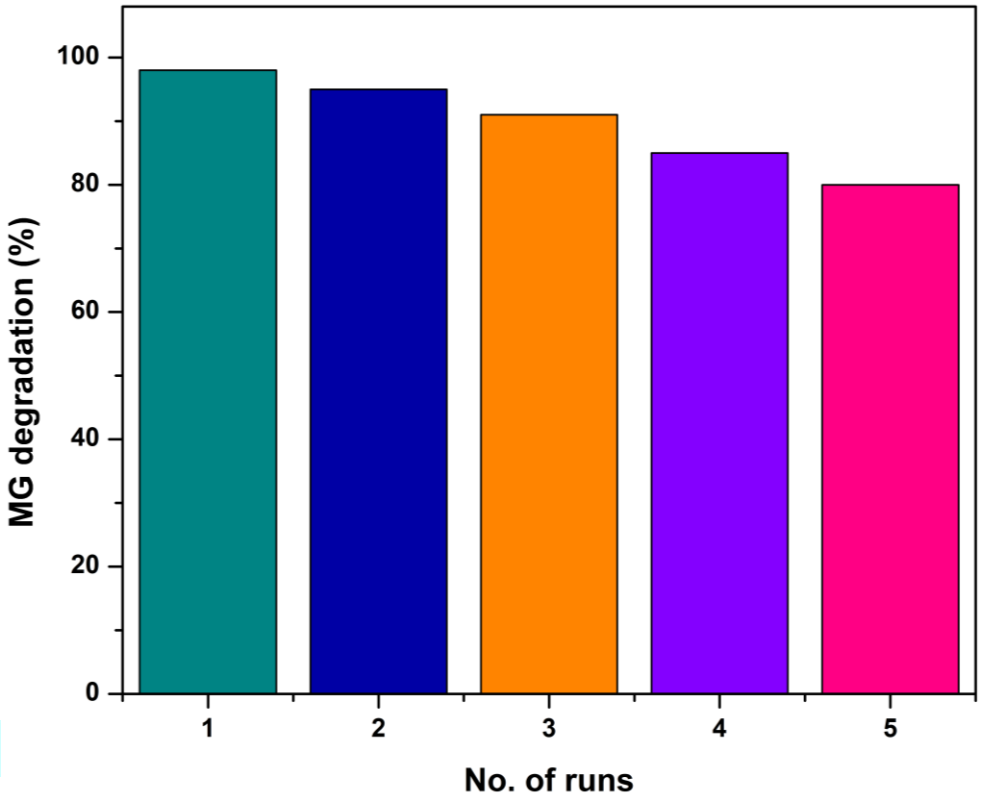

Fig.12: recycling test of prepared ZnS-RGO composite

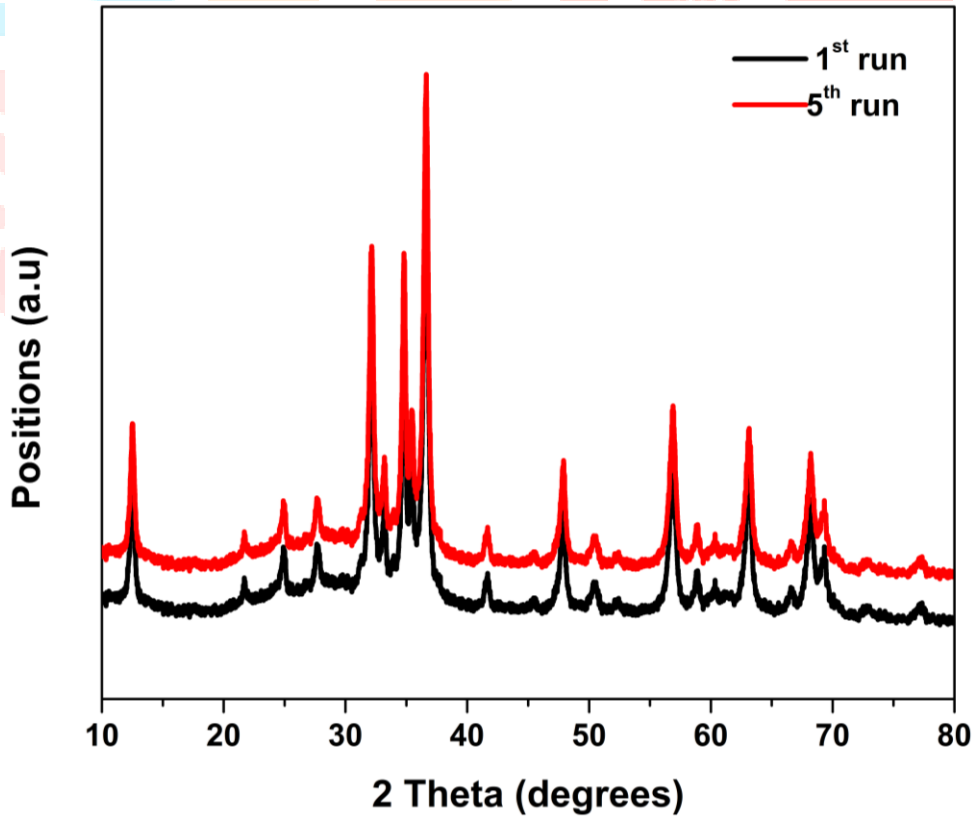

Fig.13: Stability of prepared ZnS-RGO composite

3.11 Antimicrobial activity

The ZnS-RGO composites and pure ZnS were tested with pathogens such as *E.coli, S.aureus, S.typhi and V.cholera*. The antimicrobial performance of prepared ZnS and ZnS-RGO composites were performed over the pathogens using the standard of Chloramphenicol. The obtained results found that less zone of inhibition was achieved by tested ZnS. The maximum inhibition occurred by ZR-2 composite than ZR-1 composite over the tested pathogens as the insertion of RGO with ZnS. Table 1 shows the zone of inhibition of tested ZnS and ZnS-RGO composites on different pathogens. The tested ZR-2 composite exhibited a greater inhibitory effect recorded against *E.coli* (13 µg/mL) and gram-positive bacteria is observed (Fig.14) to be so effective than gram-negative. *S.typhi* exhibits greater inhibition of its growth rate using tested composites.

Table.1: Zone of inhibition (mm) of prepared samples

Organism	**ZnS**	**ZR-1**	**ZR-2**	**Standard (µg/mL)**
E.coli	7 ± 0.1	11 ± 0.2	13 ± 0.5	26 ± 0.3
S.aureus	8 ± 0.5	10 ± 0.2	12 ± 0.2	28 ± 0.2
S.typhi	7 ± 0.2	9 ± 0.5	13 ± 0.3	27± 0.3
V.cholera	5 ± 0.3	7 ± 0.1	9 ± 0.1	28 ± 0.1

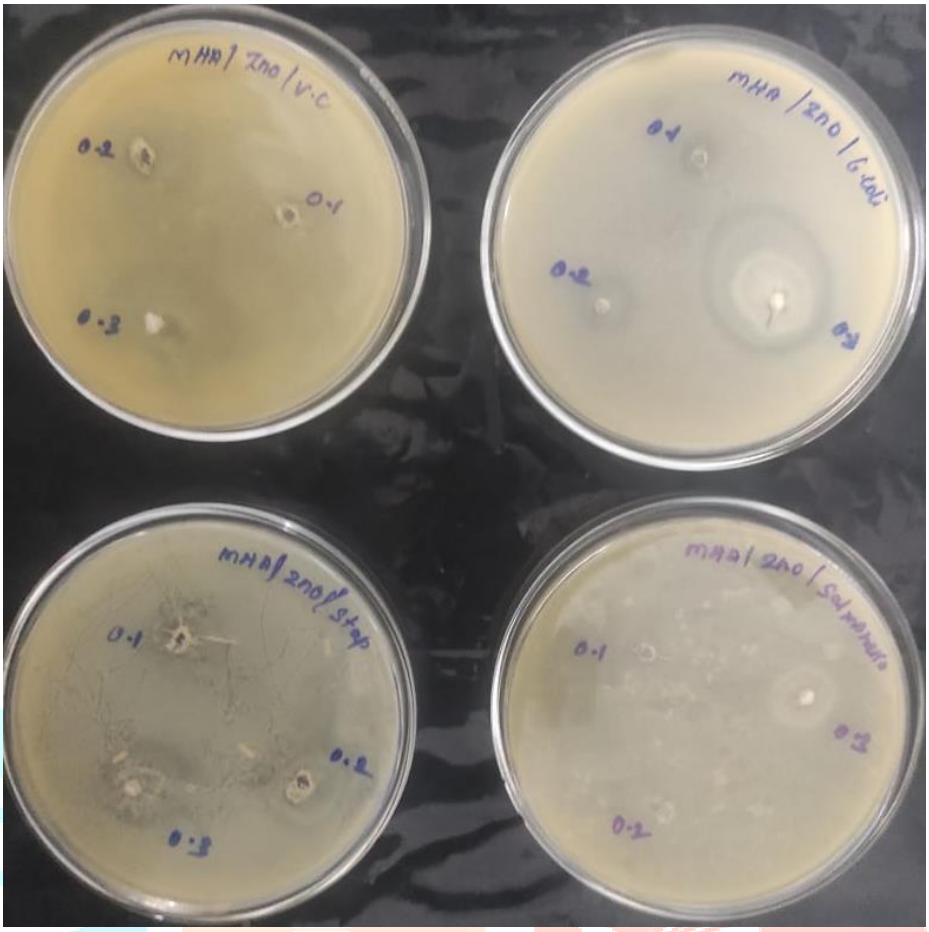

Fig.14: Antimicrobial activity of prepared ZnS-RGO composite

Conclusion

Herein, we address the water pollution and its causes mainly by malachite green (MG) dye and microorganisms. To overwhelm the solution, we prepared a composite with ZnS and RGO by co-precipitation approach. The prepared materials are well confirmed with various sophisticated instruments and studied their physical, chemical and optical properties. The photocatalytic activity of prepared samples was executed by the photodegradation of MG dye aqueous solution under visible light irradiations. The results stated that prepared blend ZnS composite shows lesser in size compared to other material which declares that ZR-1 have a greater surface area that can accommodate more dye molecules on the surface. The ZR-2 composite degraded MG dye completely in 180 min and the optimum conditions are pH-9, 0.03g catalyst dose and 10 ppm MG dye concentration. The ZnS-RGO composites and blend ZnS were tested with pathogens such as *E.coli*, *S.aureus*, *S.typhi and V.cholera*. Initially, the antimicrobial performance of prepared ZnS over the pathogens at the standard of Chloramphenicol was studied and found less zone of inhibition achieved. The maximum inhibition occurred by ZR-2 composite than ZR-1 composite over the tested pathogens as the insertion of RGO with ZnS. Hence, a current composite can be applied to cleaning the wastewater on a large scale with cost-effective and eco-friendly.

References

[1] Botsa, S.M., Basavaiah, K. Fabrication of multifunctional TANI/Cu_2O/Ag nanocomposite for environmental abatement, Sci Rep., 2020, 10, 14080.

[2] SM Botsa, GP Naidu, M Ravichandra, SJ Rani, RB Anjaneyulu, CV Ramana, Journal of Materials Research and Technology 9 (6), 12461-12472.

[3] Fu, H., Pan, C., Yao, W. & Zhu, Y., Visible-Light-Induced Degradation of Rhodamine B by Nanosized Bi_2WO_6. J. Phys. Chem. B, 2005. **109**: p. 22432–22439.

[4] Yeh, R. Y.-L., Hung, Y.-T., Liu, R. L.-H., Chiu, H.-M. & Thomas, A., Textile wastewater treatment with activated sludge and powdered activated carbon. Int. J. Environ. Stud, 2002. **59**: p. 607–622.

[5] Alinsafi, A., Electro-coagulation of reactive textile dyes and textile wastewater. Chem. Eng. Process. Process Intensif, 2005. **44**: p. 461–470.

[6] Métivier-Pignon, H., Faur-Brasquet, C., Jaouen, P. & Le Cloirec, P., Coupling ultrafiltration with an activated carbon cloth for the treatment of highly coloured wastewaters: A techno-economic study. Environ. Technol, 2003. **24**: p. 735–743.

[7] Malik, P. K. & Saha, S. K., Oxidation of direct dyes with hydrogen peroxide using ferrous ion as catalyst. Sep. Purif. Technol, 2003. **31**: p. 241–250.

[8] Dutta, K., Mukhopadhyay, S., Bhattacharjee, S. & Chaudhuri, B., Chemical oxidation of methylene blue using a Fenton-like reaction. J. Hazard. Mater., 2001. **84**: p. 57–71.

[9] D.F. Oills and H. Al-Ekabi, Photocatalytic Purification and Treatment of Water and Air. Elsevier, Amsterdam, 1993.

[10] M. R. Hoffmann, T.S., Martin, W. Choi and D.W. Bahnemann, Environmental applications of semiconductor photocatalysis. Chem. Rev., 1995. **95**: p. 69–96.

[11] P. K. Malik, S. K. Saha Sep. Purif. Technol. (2003) 31: 241–250.

[12] Reza Moradi, Mahdi Hamidvand, Amin Ganjali Russ. J. Phys. Chem. (2019) 93: 1133.

[13] D.F. Oills and H. Al-Ekabi, Photocatalytic Purification and Treatment of Water and Air. Elsevier, Amsterdam (1993).

[14] R. B. Anjaneyulu, B. S. Mohan, G.P. Naidu, R. Muralikrishna, Phys. E:Low dimens. Sys. and Nanostru. (2019) 108: 105-111.

[15] D. I. Kim, S. H. Choi, G. O. Park, J. Mater. Sci.: Mater. Electron. (1998) 9(1): 31-34.

[16] SJ Rani, SM Botsa, Russian Journal of Physical Chemistry A, 2020, 94, 392–400.

[17] Chen, W. T.; & Hsu, Y. J.; L-Cysteine-Assisted Growth of Core-Satellite ZnS-Au Nanoassemblies with High Photocatalytic Efficiency. Langmuir, 2010. **26**(8): p. 5918-5925.

[18] AG Raju, BD Rao, G Himabindu, BS Mohan, J Mater Res Tech., 2022, 17, 2648-2656.